



A 3D-printed modular implant for extracellular recordings

Dorian Röders^a, Jesus J. Ballesteros^a, Celil Semih Sevincik^b, Sara Santos Silva^a, Luca Bürgel^c, Bilal Abbas^c, Yannik Neukirch^a, Roland Pusch^b, Jonas Rose^{a,*} 

^a Institute for Cognitive Neuroscience, Neuronal Basis of Learning, Department of Psychology, Ruhr University Bochum, Bochum, Germany

^b Institute for Cognitive Neuroscience, Department of Biopsychology, Faculty of Psychology, Ruhr University Bochum, Bochum, Germany

^c Institut für Produkt und Service Engineering, Chair of Hybrid Additive Manufacturing, Faculty of Mechanical Engineering, Ruhr University Bochum, Bochum, Germany

ARTICLE INFO

Keywords:

Implant
3D-printing
Extracellular recording
Operation

ABSTRACT

Background: Chronic implants for neural data acquisition must meet several criteria that can be difficult to integrate. Surgical procedures should be as short as possible to reduce unnecessary stress and risks, yet implants must precisely fit to the location of interest and last long periods of time. Implants also must be lightweight but stable enough to withstand the subject's daily life and experimental needs.

New method: Here we introduce a novel, 3D-printed and open-source modular implant. Our modular design philosophy allows altering parts of the implant either before implantation or later, during the course of experiments. The implant consists of a base individually designed, for instance using an MRI of the subject for an exact skull fit. This base remains permanently on the subject and can contain multiple sites for craniotomies, microdrives and head stage connectors. All movable components (drives with probes, connectors, reference/ground points) are securely screwed onto this base, allowing for replacement and recovery.

Results: After implantation of the bases, self-made microdrives carrying commercial silicon probes were implanted. Once the experimental goals were achieved, they were recovered for further use. Should the quality of the data decrease during the experimental period, the components were replaced, allowing for the experimentation to continue. On an exemplary free-moving subject, under wireless electrophysiological data collection, we reliably obtained single and multi unit data up to 86 days after a silicon probe implantation. In this specific case, after this time we successfully substituted the components and collected similar quality data for additional 11 days.

Comparison with existing methods: Our approach allows to remove, reposition and exchange components during minimally invasive procedures, not requiring new incisions, bone drilling (unless new craniotomies are planned sequentially) or removal of dental cement or glue structures. Splitting complex implantations into multiple shorter procedures reduce the risks inherent to long surgical procedures. A careful plan of action allows to re-use and reduce subject's usage.

Conclusion: This novel approach reduces the duration of surgical procedures. It allows for minimally invasive follow-up procedures, including component replacements between experiments. The design is stable, proven to yield good results, in a very long-term period. This approach increases the chance of successful long experimental paradigms, and help reducing the use of subjects.

1. Introduction

Recording neuronal action potentials and local field potentials (LFPs) via intracranial electrodes is one of the many ways neuroscience is gaining insight into the functions of the brain (Jun et al., 2017; Buzsáki, 2004; Guillory and Normann, 1999). Technical developments in the field have led to many improvements of the electrodes themselves, often

resulting in a much higher channel count (Steinmetz et al., 2018). Yet, there is still a multitude of technical difficulties faced by researchers, especially in case of long term, chronic, implantations. One may find a deterioration of recording quality over time or mechanical failure of components, such as loosening of wires, clogging of small connectors or even a complete destruction of recording components by the subjects, which can occur easily in group housed animals. In the most unfortunate

* Corresponding author.

E-mail address: Jonas.Rose@ruhr-uni-bochum.de (J. Rose).

<https://doi.org/10.1016/j.jneumeth.2025.110407>

Received 28 October 2024; Received in revised form 4 February 2025; Accepted 20 February 2025

Available online 27 February 2025

0165-0270/© 2025 The Author(s). Published by Elsevier B.V. This is an open access article under the CC BY license (<http://creativecommons.org/licenses/by/4.0/>).

cases, this can result in probe loss, complete explantation or even euthanasia of the animal. Additional challenges can arise if the experiments take on a network-level perspective which may require data collection from multiple target structures in parallel or combining causal manipulations of one target area with recording from another area. Especially in experimental designs requiring long term training or data collection, as is often the case when exploring complex cognition, an efficient and easily adaptable procedure may be necessary to achieve these goals.

There are already commercially available premade implants, which remove the need for creating a large dental cement structure, for example the 'dDrive' (NeuroNexus, Ann Arbor, USA) or the 'Neuropixels drive' (ATLAS Neuroengineering, Leuven, Belgium). These implants comprise a probe, a microdrive and a connector for a headstage. Some publications also show implants with repositionable and/or reusable microdrives. Vöröslakos et al. designed an implant with a circular repositioning system around a region of interest for rats (Vöröslakos et al., 2021). This system includes a faraday cage, a stainless steel microdrive and a cylindrical chamber printed with a resin 3D-printer. The microdrive can be fixed on multiple positions on the wall within the chamber to sample the entire region. It also allows for the use of multiple drives at the same time. A similar system, intended for the use in the marmoset brainstem (Pomberger and Hage, 2019), also allows for repositioning the drive in a circular chamber, but uses a sturdier cylinder made out of titanium, safeguarding against manipulation attempts of the monkeys. The flex-drive (Voigts et al., 2013), consisting of a 3D-printed housing for a multi microdrive system, designed not to move entire probes but to adjust the depth of single electrodes independently into the brain of rats, allows for a more fine-grained control of electrode position. The same approach is followed by a system, to study pain related neural areas in rats (Ma et al., 2019). The 'rat hat' (Allen et al., 2020) has a 3D-fitted shape to variable positions on the rat's skull, where probes can be inserted in several positions around an area of interest. The 'rat hat' does not require a stereotactic apparatus to fixate it to the rat's skull. The exact 3D-fit automatically positions the implant at the correct location.

Our new implant design is aimed at combining multiple aspects of previous designs, producing an implant ideally suited for the work with our specific lab animals, while being still compatible with more commonly used animals like mice and rats. Our lab mainly performs long term electrophysiological recordings in corvid birds and in pigeons, commonly working with individual animals for several years. The implants are also subject to more movement stress than those of rodents, as the primary way of measuring behavioral output in birds is through screen pecking. Birds also tend to do ballistic head shaking movements, which can further increase the stress on the implant. A modular implant, where individual pieces can easily be replaced, is ideal for such species. To keep the system affordable and customizable we opted for resin 3D-printing as not to rely on third party manufacturers with more costly metal 3D-printing.

Our approach aims to reduce strain on subjects in line with the 3 R principle (reduce, replace, refine, (Lewis, 2019)), to gain more flexibility in data-acquisition and to reduce technical challenges. Our implant consists of a 3D printed baseplate that is fitted to the animal's skull. Only this base is attached permanently to the skull, all other components are fastened to this base. Creating an exact fit to the skull from an MRI or CT scan (as it is common in non-human primate research (Psarou et al., 2023; Overton et al., 2017)), decreases the likelihood of the implant dislocating from the skull, while simultaneously reducing the number of skull screws and amount of dental cement necessary for secure attachment. Should customization to an individual subject not be necessary or practical a standard 3d skull model can alternatively be used. With our modular approach to implantation, individual components can later be moved, removed, or replaced when needed. This only requires minimally invasive procedures without reworking bone-attachments. It greatly reduces the time needed for succeeding operations and therefore reduces the likelihood of complications and allows to easily record from

new locations or exchange an electrode for instance with a light guide for optogenetics.

The usual procedures for implanting microdrives with attached electrodes, are in short (Bilkey et al., 2003):

1. Anaesthetizing the animal.
2. Exposing the skull.
3. Drilling craniotomy sites.
4. Inserting the electrodes.
5. Building a dental cement and skull screw construct around the microdrive and wiring.

This results in a fixed construct of dental cement, permanently attached to the skull. Using a microdrive will typically allow electrodes to move along the dorsoventral (DV) axis. However, the electrodes are often locked in the anteroposterior (AP) and mediolateral (ML) axes. Should problems arise with the recordings, identifying the problem can be challenging since the individual components are often embedded in dental cement and therefore hard to access. Should the implant need to be exchanged or repositioned, the dental cement must be removed, often in lengthy or risky procedures.

The adaptable base design of our implants can be fitted to individual animals, species, or brain regions. It is prepared for multiple configurations of elements and placed via a stereotactic technique on the skull. On top of this base, flexible repositioning of the microdrive along the AP and ML axes is possible. Therefore, multiple regions of interest could be sampled with a single implant, at the same time or on successive experiments. The microdrive and probe are then sealed from the environment with a protective cap. Dedicated elements to house the connectors can simply be screwed to the base over unused spaces, and repositioned if required, thus drastically reducing the implant size and weight. By 3D-printing and pre-assembling most of the implant components, a considerable amount of time for the procedures can be saved. 3D-printing of implants, with a precision in the 25 μm range, also saves materials and weight, reducing the use of dental cement. This also downsizes the implant to be advantageous for its use in smaller or flying animals. Any component can be modified by laboratories for specific purposes through 3D design and post-print manufacture. Although 3D-printing at high resolution takes time, it does not involve active work and can be fully automated. Importantly, by precisely manufacturing all drive components, this process does not need to be performed during surgery.

Our implant design addresses challenges of long-term avian electrophysiological recordings. Through a modular design of not only the physical implant, but also individual part files with modular components, we offer a customizable solution. This approach facilitates precise fitting to reduce the risk of implant loss and enables easy adaptation for subsequent experiments, as detailed in the following methods.

Implants and equipment shown in the publication are available (<http://gitlab.ruhr-uni-bochum.de/ikn/modular-implant>) and will be successively updated with new projects from this and other labs.

2. Material and methods

2.1. Animals

We tested the procedure on 17 pigeons (*Columba livia*). The pigeons were housed in individual cages. During the recording procedures the animals were on a controlled food protocol, never below 80 % of their ad libitum weight, and they always had free access to water and grit in their home cages. All experimental procedures and housing conditions were carried out in accordance with the National Institutes of Health Guide for Care and Use of Laboratory Animals and were authorized by the national authority (LANUV) and agreed with the EU directive 2010/63/EU concerning the use and care of experimental animals.

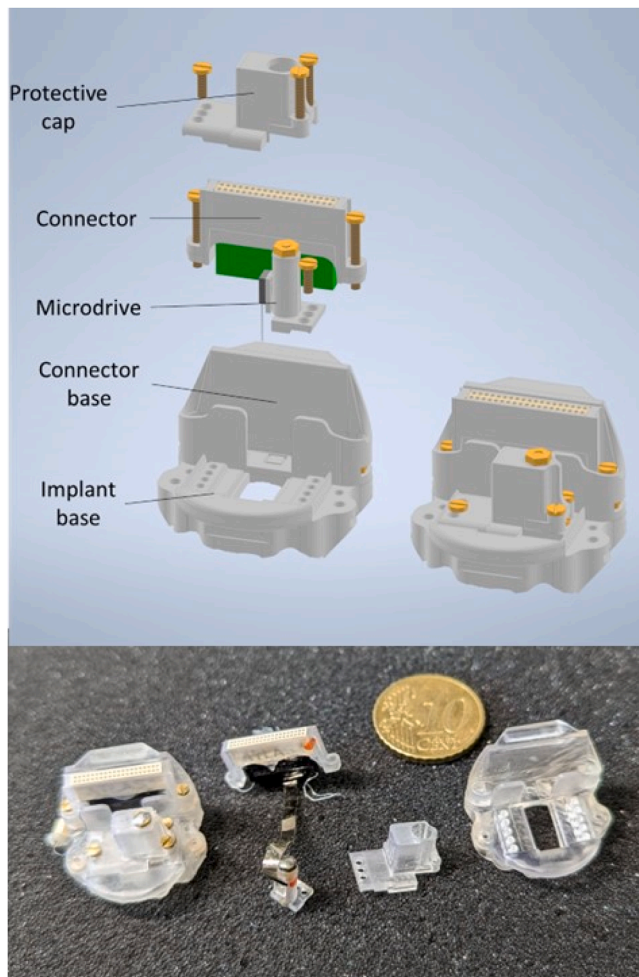


Fig. 1. Explosion sketch of the entire implant together with a collapsed version and a physical implant. The placement of all screws and parts that are used in a successful operation are indicated, parted into the three major steps of the operation: implanting the baseplate, fixing the drive and covering it with the protective cap.

2.2. Head models

The described implants are either fitted to a 3D-skull model created from an MRI of PFA fixated bird heads or to a 3D-pigeon skull model supplied by Jones et al. (2019). All implant parts were designed with Autodesk Inventor (Inventor Professional 2023, Autodesk Inc, San Francisco, California).

2.3. Electrophysiology recordings

The success of the chronic implantations was measured by the yield of putative single neurons from recordings made on a close-to or actual experimentation basis. The recordings were done with 32 channel silicon probes (E32+R-50-S2-L10 PEDOT, ATLAS Neuroengineering bvba, Leuven/A1x32-Poly3-10mm-50-177, NeuroNexus Technologies, Inc, Ann Arbor, MI, USA). Wired recordings were performed before the freely moving recordings, to control for probe positioning and stability of signals. Under these conditions, the signal was amplified, filtered, and digitized using Intan RHD2000 headstages and an USB-Interface board (Intan Technologies LLC, Los Angeles CA USA). Only after the signal was stable, we proceeded to perform wireless recordings. Here the acquisition was done with a Spikelog 64 C logger, with a sampling rate of 30k Hz, controlled by radio commands from the synchronizing transceiver (Deuteron Technologies Ltd, Israel), connected via USB to the host

computer. The high-pass data (filtered between 500 – 5000 Hz) was then pre-processed with custom MATLAB code, putative clusters of action potentials were extracted and sorted via Kilosort 4, and then manually inspected with the Phy graphical user interface (Pachitariu et al., 2016).

2.4. Testing the microdrive

A key factor to achieve good results in chronic recordings was the reliability of the probe's trajectories while in the brain tissue. The microdrives' trajectory accuracy was tested via measuring the displacement from the two perpendicular axes while travelling on the dorsoventral direction. For this, as the silicon probes of interest were 10 mm long, equally long metal needles were attached to five separate drives and tested by moving them 5 times in 500 μ m increments. Displacement from the expected trajectory was measured (at the tip of the needle) in micrometers, using a VHX Digital Microscope Multi Scan (Keyence, Osaka, Japan) under 200x magnification. We moved the drive by doing two full turns to measure the dorso-ventral accuracy. This was done with five microdrives, four times for each drive.

2.5. Implantation

All essential parts for our modular implant are given in Fig. 1. In the following we will describe how to attach the baseplate onto the skull of the animal, attach the microdrive with the probe and connector, and finally secure everything with the protective cap.

The first steps of an operation with a 3D-printed implant are very similar to those of any other implant operation. Anesthesia should be similar to other procedures and fit each institution's protocols (Pusch et al., 2023). Nonetheless, it is worth considering that operations with our design tend to be quicker than the ones that require large amounts of dental cement, since most parts of the implant are prebuilt.

Once the animal is fully anesthetized and the skull properly exposed, it is ready to receive the base (Fig. 2). The key is to make it fit to the shape of the animal by precisely locating the craniotomy site(s) over the desired stereotactic coordinates for the recording site. This way, the access to the brain will be located under the open space and the rest of the base should fit the skull around it. For this purpose, our stereotactic adapter is screwed onto the implant base (Fig. 3). The base can then be connected to the stereotactic apparatus via a mounting rod, connected to the stereotactic adapter. The set is then located over the skull at the desired coordinates. The outline of the craniotomy site and implant base can be drawn with a pencil on the animal's skull, by lowering the implant base on the skull and outlining the borders of the craniotomy window. The intended skull screw positions are also marked, around the delineated outline, and the location of the reference screw is marked by inserting a mechanical pencil through the corresponding nut. Positioning the stereotactic adapter at the desired electrode position will place the implant base on the correct location for the window to implant the probe. In the example pictures, this location is over the hippocampus of the pigeon at ML \pm 0.5 mm (both hemispheres are accessible) and AP 6 mm.

After outlining the implant and craniotomy positions, the implant base can be lifted to leave space for working on the skull. A few holes are drilled within the marked area into the first layer of the skull (this step is specific to the multilayered skull of birds). These holes are filled with dental cement to serve as anchor points, and the rest of the area is coated with a very thin layer of dental cement (Rose, 2018). Care should be taken to avoid covering the craniotomy area or any of the screw places with this layer. Once the cement layer is dry, a thin continuous line of viscous glue (Loctite 3090, Loctite, Düsseldorf, Germany) is placed on top, along the outline of the implant. Again, we advise to be careful by leaving the areas that will be drilled free from glue. Then the implant is lowered on to the glue, and the connection to the stereotact should not be removed until the glue has hardened (following the manufacturer instructions on hardening times has proven to be reliable to us).

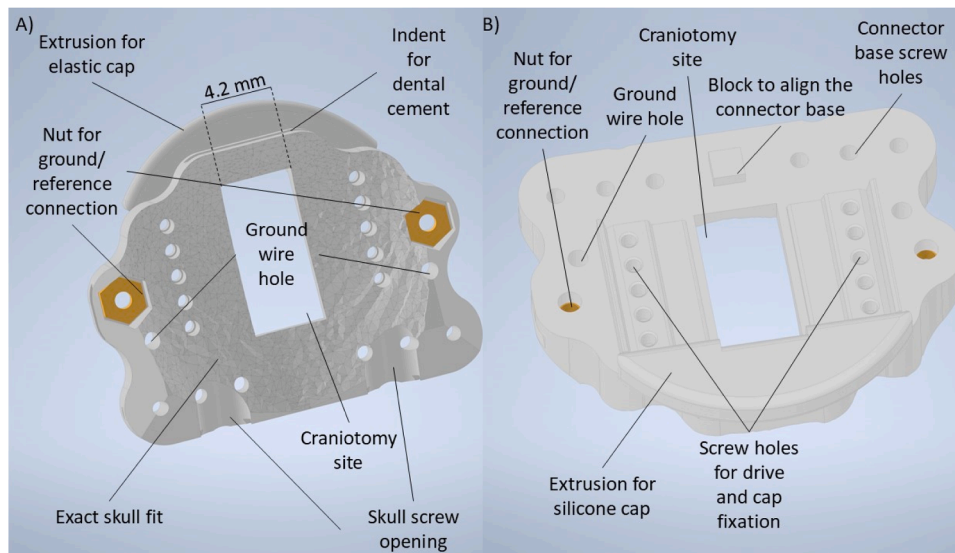


Fig. 2. Implant base. The implant base is fitted to the skull of the animal. It contains screw holes for all parts of the implant that are added on top. This part is glued to the skull with viscous glue (see main text) on top of a thin dental cement layer. The craniotomy site (located in the midline, in this particular example) is large enough to encompass the region of interest and leaves additional maneuverability space. Indents for dental cement create a more stable build. In the bottom view (A), openings for the skull screws and the exact fit to the skull surface are visible. The screw, connecting the ground to the cable from the headstage, can be pressed on tighter owing to the nuts in the baseplate.

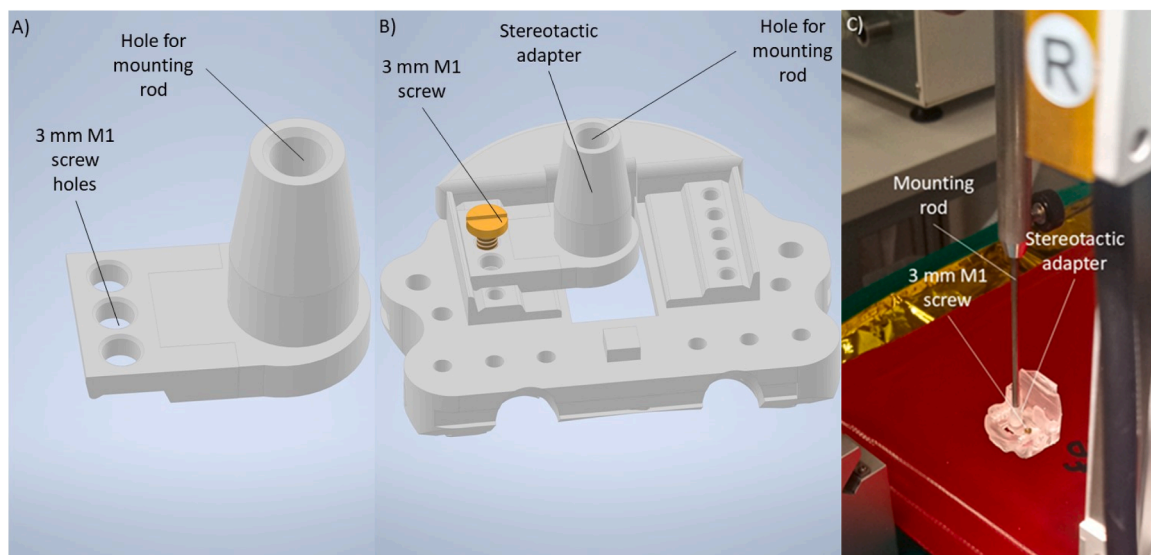


Fig. 3. Implant base with stereotactic adapter. The stereotactic adapter (A) enables placement of the base plate (B) in relation to the region of interest, being located at the empty window. See also real life picture (C). The hole at the top of the adapter serves as a connection to the stereotact. When the adapter is connected to the stereotact and implant, moving it to the coordinates of the region of interest also moves the entire implant to the correct location. The size of the stereotactic adapter also accounts for the thickness of the probe and the glue.

Skull screws and ground/reference screws can be placed within or around the implant, prepared with wires as desired, and covered with dental cement as necessary (the back of the implant has indents for closely placed screws, Fig. 2). The intention of the external layer of dental cement and screws is to further reinforce the structure, as well as sealing the outer border of the base. This layer does not need to be thick. Our grounding involved a copper wire with insulation stripped at the tip, tied to a ground screw in the back of the skull. A reference screw was placed through the base at the nut for ground/reference connection (Fig. 2) with another copper wire attached. The nut serves as a tighter hold for a reference than a thread cut into the hardened resin could be. These two wires belong to a small 2-pin (or 4-pin) connector (Omnetics part 79602-001) which is then cemented to the back of the base. Here,

we can plug the mentioned matching connector soldered to the electrode's reference and ground wires. If the glue is not yet dry, additional waiting time is necessary before removing the stereotactic adapter from the implant.

Once the base is securely attached and all the surrounding work is done, the stereotactic guide can be removed by first unscrewing the M1 screw and then lifting up the stereotactic arm. Any empty space between bone and implant base surrounding the craniotomy is sealed with dental cement to create a smooth seal. Then, the craniotomy can be drilled through the baseplate window. Once the craniotomy is open, it is important to seal the skull layers to avoid or delay regrowth. This is especially important in bird skull, as it is composed by two layers of dense bone with a more or less wide cancellous bone in between. The

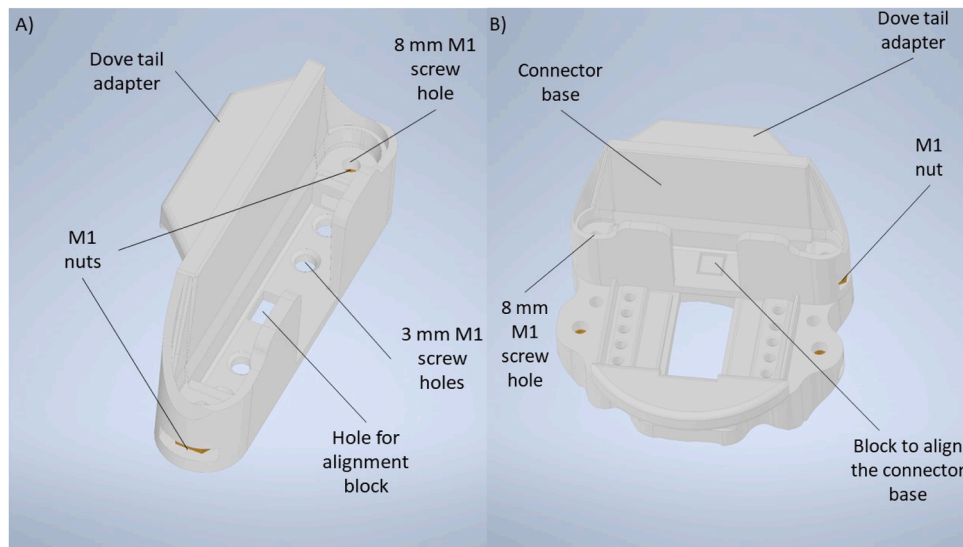


Fig. 4. Connector base and connector base on the implant base. The connector base (A) later contains the connector house (see Fig. 1). This, in turn, contains the connector of the probe. While the connector base is a detachable part, which can be switched out or turned depending on region, it can also be directly printed onto the implant base (B) or screwed on before implantation.

cement is needed to cover the edges of the two layers and to seal the spongy space in between. At this point, the cement could flow on top of the dura, therefore special care was taken during this step, and small steps of setting and polymerizing cement are recommended. A tiny piece of wet gauze could help to avoid the cement polymerizing directly on top of the dura, and any cement running on top of the gauze would be easier to remove without damaging the dura. The dura can be now removed, if required. The brain is protected with Dura-Gel (Cambridge Neurotech, Cambridge, UK), which needs to cure for a day before a probe should be inserted. For insertions within one surgery, a piece of gauze and saline solution kept the brain wet and then only after probe insertion the craniotomy was filled with vaseline. Finally, if the probe will be located on another day, a rigid lid can be placed on top to cover the window.

The base needs a space where the probe connector can be placed. For this purpose, our connector base can be screwed onto the implant base via 3 mm M1 screw holes (Fig. 4). Other options, since this piece is normally not in the way of any important procedure, are to directly print it as a single piece with the implant base (if it will not need to be moved) or to have it screwed on the implant base in advance. It is important to highlight that this piece, like the microdrive itself, can be eventually replaced if broken, or moved to another position, if the base has been planned for it. As an example, two craniotomy sites could exist, to record from two different brain areas at two different stages of the experimentation. The connector base could initially be located on top of the inactive craniotomy site and be moved on top of the previously used site to free the new one.

2.6. Preparing the probe

The probe itself is, normally, the most expensive and fragile part of the entire implant. Gluing the probe to the shuttle and implanting it requires precision and care. For assistance with this step, the probe glue station (Fig. 5) ensures a smooth procedure.

A stereotactic mounting rod, for instance the Neuronexus insertion tool (IST, NeuroNexus Technologies, Ann Arbor, MI, USA), is screwed into our stereotactic guide (Fig. 5B). The stereotactic guide is designed so that the probe, once glued to the microdrive, matches its desired stereotactic position. The stereotactic guide carries the microdrive, which is inserted from the bottom by exerting a light pressure. The relative flexibility of its walls allows for this easily, and for a stable holding during the procedure, as well as for a smooth release once the

microdrive is fixated in its final position.

Our connector house holder (Fig. 5B) is designed to hold the connector house for the electrode connector piece. The connector house holder is also carried by the mounting rod, which is inserted through a thread into the stereotactic guide. It is important to leave sufficient space between the connector house holder and stereotactic guide to fit into the glue station. In this position, the connector house holder can be secured by screwing an M2 screw through a small hole below it (Fig. 5C). This design shows a single standard 36-pin Onmetics connector, but other of our implant designs feature two of such connectors, for two independent probes in parallel. Modifying the connector house to hold 64 channel connectors, connectors from other brands, or modifying the entire implant to hold other probe types like Neuropixels probes (Neuropixels, Leuven, Belgium) is certainly possible, but it would require dedicated and careful design and testing.

The next step is to insert the electrode connector piece into our connector house and to glue it in. The connector needs to be checked for large extrusions due to the glue already applied by the manufacturer; if so, these need to be sanded down. One small drop of viscous glue is applied to the electrode connector piece. Subsequently, the connector house is slipped over the connector. After sufficient drying time, a more fluid glue (Loctite 406, Loctite, Düsseldorf, Germany) is applied between the connector and connector house to close all possible gaps between the two parts. A tightly glued connection is essential here, as there is force applied to the connector while plugging and unplugging the headstage at every recording session.

Now, the guide railings (Fig. 5D) can be placed in position over the microdrive. They are fixed by exact fit and should help to place the probe in a constant position over the microdrive's shuttle. At this point, all elements should be in place as shown, and the probe is ready to be glued.

The probe is removed from its packaging following the vendor recommendations. The connector and its house are slipped into the connector house holder while holding the probe. It is possible to screw the connector house in, which could be useful if a headstage is connected before implantation, to test the probe. In this case, it provides an additional hold and avoids strain on the cables while pulling out the headstage. Finally, a small drop of viscous glue is placed on the shuttle (Fig. 5B) and the probe is carefully placed on top. The probe can be aligned using the guiding railings and the guide line (Fig. 5D). Most probes have 1–4 cables with deinsulated ends, coming from the

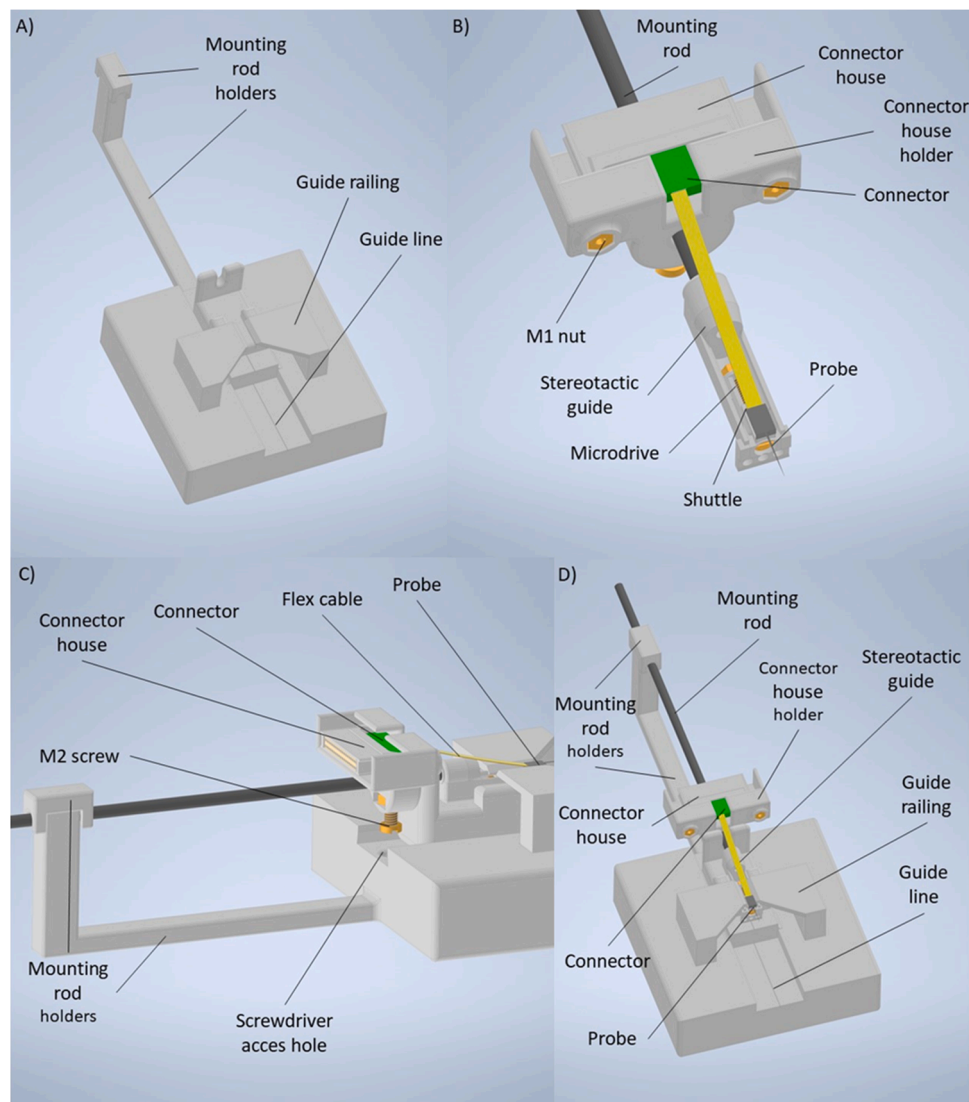


Fig. 5. Probe glue station. The probe glue station (A) serves as an aid in gluing the probes to the microdrives in the correct orientation without breaking them. The figure depicts all parts and their assembled view. The mounting rod is prepared to carry the connector, its housing, the microdrive and its guide (B, with the probe already glued). The base holds the insertion tool at two points, that are shaped to hold it still (C). Once the probe is glued (D), the mounting rod is easily removed from the station, placed on the stereotactic apparatus, and used to place the microdrive on the planned location at the implant base.

connector, dedicated to reference and grounding connections. These can be soldered to a pin connector (Omnetics part 79602–001), which is later connected to ground and reference on the implant.

The microdrive, with the probe attached, can now be placed in the stereotact by connecting the mounting rod used at the time of gluing them (Fig. 5B). Once there, we proceed with lowering the whole construct at the desired coordinates. When the coordinates are well matched, the three M1 screw holes (Fig. 6B) are automatically placed over the ones in the implant base. The connector house holder can be moved downward by lightly unscrewing the 5 mm M2 screw (Fig. 6B). This allows the connector house (Fig. 7A) to be removed without ripping the flexible cable connecting it to the probe. The connector house is then fastened in the connector base via two 8 mm M1 screws (Fig. 7B), with the extrusion in the connector house facing the probe. The ground and reference wires can be attached as described above. Note that attaching the connector house to the connector base and attaching the microdrive to the base can be performed in any order, but having everything in place before inserting the probe in the brain reduces the chance of damaging the probe or the tissue.

Now, the microdrive can be screwed into the implant base via the

middle 3 mm M1 screw hole (Fig. 6B). The alignment of the microdrive should be double-checked, since a misalignment can cause unwanted movement of the probe within the tissue when the microdrive is screwed to the baseplate. Once the microdrive is well fastened, the stereotact arm can be moved up, to free the microdrive from the stereotactic guide. This should be done while checking that the screw holds the microdrive in place and that the microdrive slides smoothly from the guide. Now, the microdrive screw is accessible and the microdrive should be stable enough to lower the probe into the brain, if required. Although it is not necessary to do so at this time, it is important to note that at this stage there is still visual access to the insertion point and it is possible to check for a proper insertion. As with other microdrives, the probe is lowered by moving down the shuttle. Moving the shuttle down is achieved by turning the screw on top of the microdrive counterclockwise with an M1 hexagonal screwdriver. It should be noted that turning the screw clockwise while the shuttle is at the highest position can break the threads in the shuttle. The same is true for turning the screw counterclockwise when the shuttle is at the lowest position.

At this point, the implant is fully operational for recording. The following steps are necessary for protecting the components from

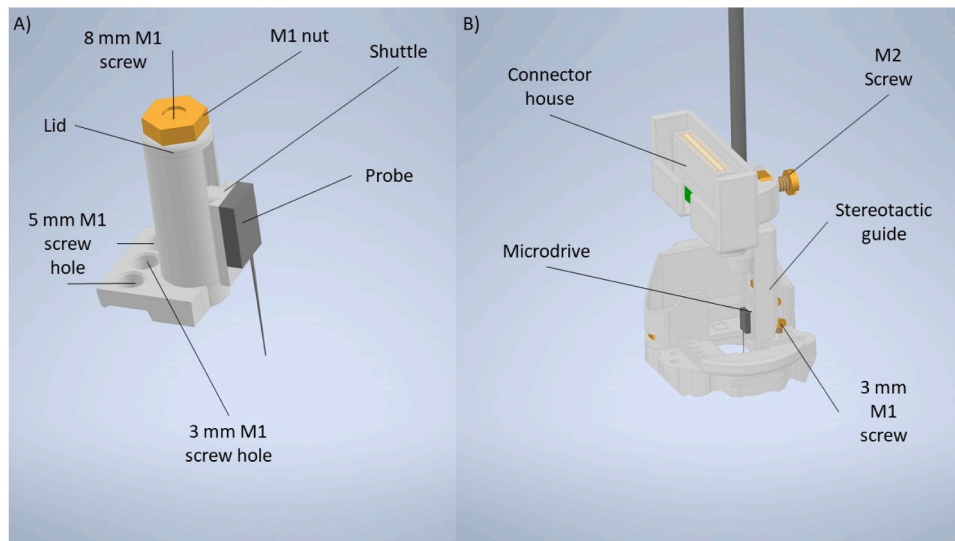


Fig. 6. Implant base with microdrive and positioning system, during placement. In the depicted case, the microdrive (A) can be positioned on three positions per side, with 1.5 mm distance between the positions, thanks to the five different possible screw places per side. The connector house is still present in its holder, before being screwed to the implant (B). The flex cable was not represented for better understandability of the image.

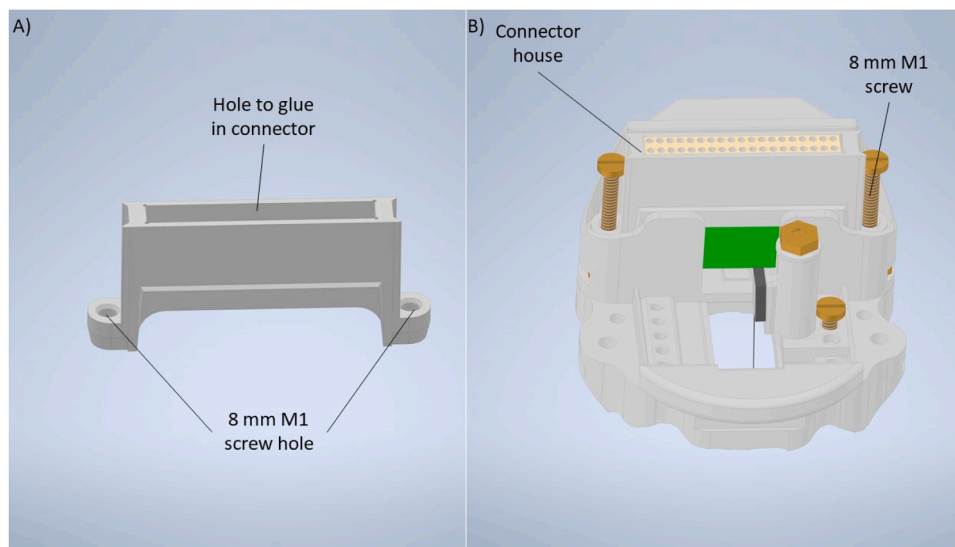


Fig. 7. Connector house and implant base with connector house. The connector house (A) contains the omnetics connector (shown only in B), into which the headstage to the acquisition system is plugged in for recording. The connector house is screwed into the nuts placed in the connector base with two 8 mm M1 screws (B). It can also be seen in the final disposition of elements once the microdrive is placed. Not shown here for better readability, but important to take in account, is the probe's flexible cable, which would run between the microdrive and the connector base, and will be covered by the protective cap later (Fig. 1).

external damage. The protective cap (Fig. 8B) is fastened over the microdrive via two 5 mm M1 screws and one 3 mm M1 screw (Fig. 8B). This piece does not need to be removed for recording or advancing the probe as it has a hole in the top to access the microdrive screw. All essential parts are now present (Fig. 1). Loose cables can be fixed via removable silicone to the implant if necessary.

2.7. Manufacturing

The 3D-printed components are all printed based on the models in Figs. 1–8. Since most 3D-printers cannot print threads accurately, they must be cut in manually. When producing threads to screw two parts to each other, only one (in case of this implant always the lower part) of the parts needs a thread. The other part requires a hole that is slightly larger than the diameter of the planned screw. If there is a thread in each of the

parts that need to be screwed to each other, the phase shift between the two threads creates a gap between the two parts. This can severely impact the spatial precision of the implant. Threads need to be cut in the screw holes for microdrive and cap fixation, the shuttle, the four inner connector base screw holes, and holes for the stereotactic adapters. Stereotactic adapters require M2 threads and everything else requires M1 threads. All other holes need to be slightly wider than the screws that pass through them. Two of the M1 nuts need to be glued from the bottom into the implant base, the other two can be glued from the sides into the connector base. It is easiest to glue nuts in the correct position by screwing in the respective screws while gluing in. We suggest using viscous glue for this step.

To manufacture the microdrive, all printed parts are first inspected with magnification and all visible support rests and obstructions are removed with a scalpel. All M1 screw holes except the one in the shuttle

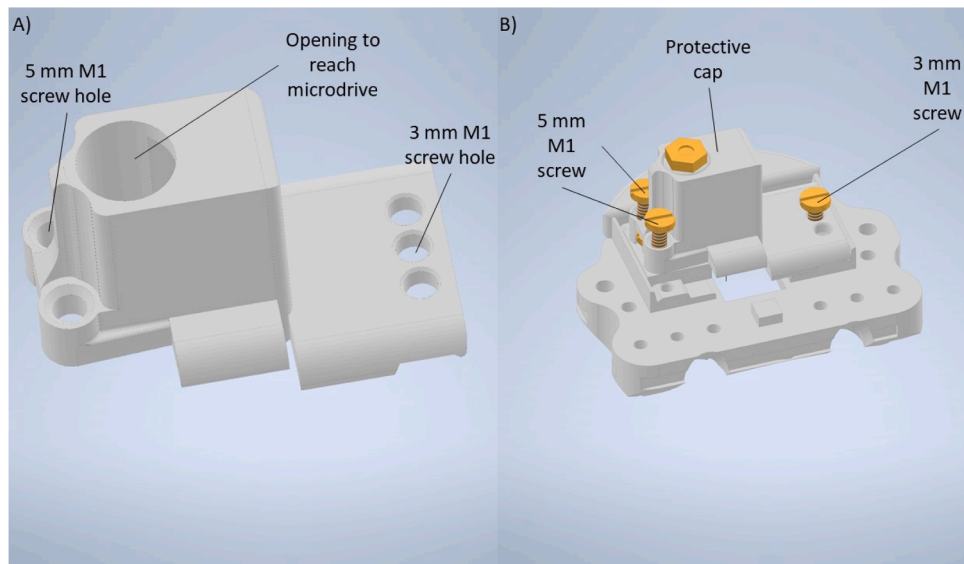


Fig. 8. Protective cap and implant base with protective cap. The protective cap (A) is screwed over the microdrive to protect the electrode and craniotomy site (B). The electrode can still be moved in the DV-axis through the hole at the top of the protective cap. The connector base was removed in this model for visual access to all important parts.

itself are drilled with a 1.1 mm drill. The shuttle is placed in the microdrive before drilling the thread of the shuttle. This helps to ensure that the thread is not tilted. The M1 screw is then inserted from the bottom through the shuttle. Small amounts of viscous glue are applied to the top of the microdrive, and the lid is pressed on top by screwing the M1 nut over it. The M1 nut that keeps the M1 screw in the microdrive needs to be soldered onto the screw. It should not be pressed onto the microdrive too tightly since it still needs to turn smoothly. It is best to move the shuttle up and down into the microdrive several times to test for proper function. Furthermore, the use of soldering fat strengthens the solder connection between the nut and the screw.

All connecting parts must be visually inspected and tested before an actual operation. This way, unfitting parts can be adjusted beforehand, mostly being manually sanded. The connector house should also be tested with a dummy connector to see if it would provide an accurate fit. All screw holes and holes for nuts that have contact to the skull surface are filled with a tiny drop of Vaseline or silicone to avoid any glue from blocking the threads when gluing on the implant. If a different 3D

printer than the one used here (Formlabs 3B, Formlabs, Somerville, Massachusetts, USA) is to be used, especially one with a lower resolution, a close inspection of the results is advised.

3. Results

Out of the 17 implanted pigeons, only one lost the implant unexpectedly, after 5 months. We believe that these time periods were enough to perform the necessary recordings for most experimental paradigms and any silicon probes could have been removed securely before the unplanned explantation of the bases.

The material used for the implant was Clear V4 resin (Formlabs, Somerville, MA, USA). There were no adverse reactions in any of the 17 implanted animals. The implant can also be printed with other Formlabs resins which have an official biocompatibility rating (BioMed Durable/Black/White/Clear Resin).

The lowest-weight implant for chronic applications we have produced weighed 3.5 g, including two silicon probes and their connectors.

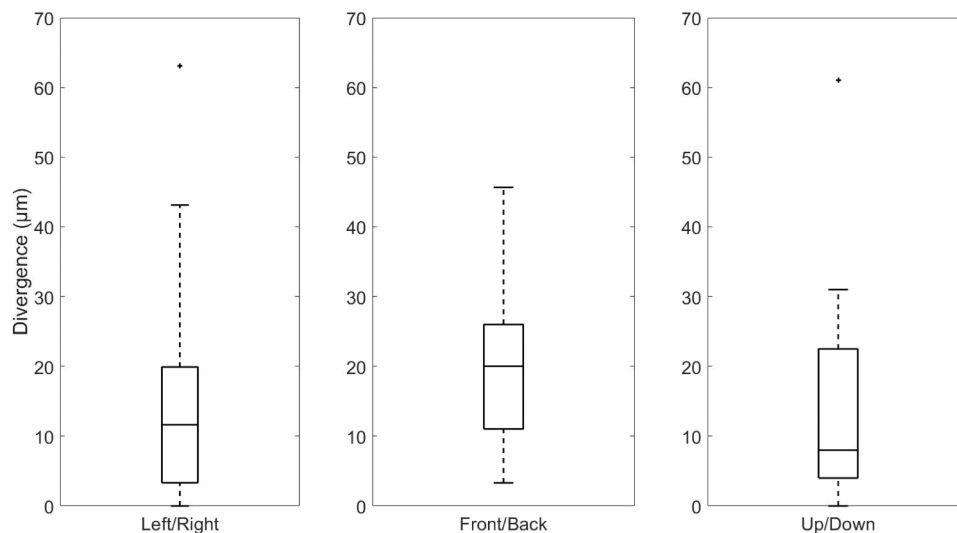


Fig. 9. Drive divergence. Five drives were turned down 500 μm , six times each, to measure displacement in the Left/Right and Front/Back axis; or two full screw turns four times each to measure the difference to the intended 500 μm movement in the Dorsal/Ventral axis.

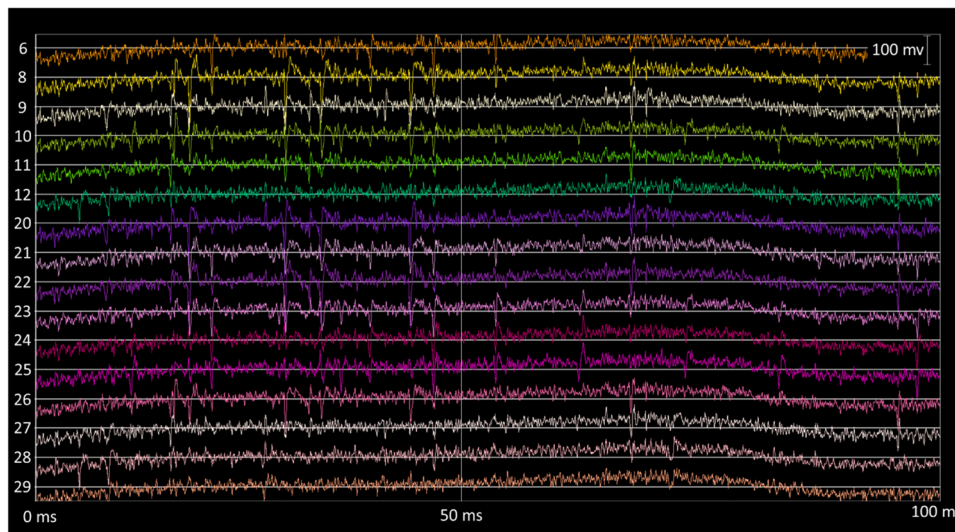


Fig. 10. Exemplary recording from a freely moving pigeon's Nidopallium caudolaterale. 100 ms recorded with Deuteron recording system. Displayed are 16 out of the 32 channels, showing action potentials often spanning neighboring channels due to the small distance between recording channels. This data was filtered between 500 and 5000 Hz for visualization purposes.

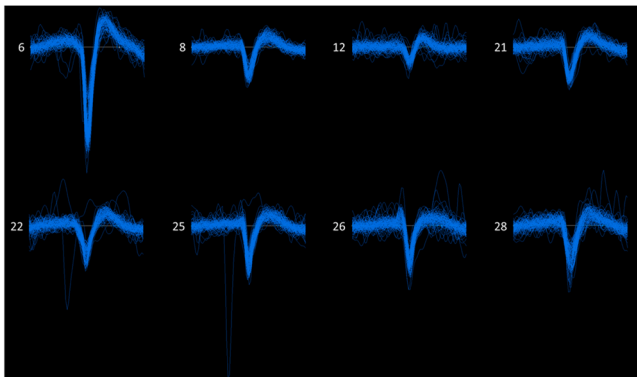


Fig. 11. Neural activity recorded from a stable long-term probe location. This figure displays 100 waveforms from eight exemplary clusters out of a total of 37, which were automatically isolated via Kilosort from the recording session shown in Fig. 10. The visualization of individual waveforms was generated by the Phy graphical user interface.

It allowed for recording in three different brain areas with up to 10 possible microdrive positions, in each hemisphere.

Our microdrive is small (9 mm×4 mm x 5 mm, H x W x D), lightweight (150 mg) and easy to assemble. No custom order products were required for assembly, it was easily placeable, removable and reusable. The microdrive has a travel of 250 μ m per full turn of the screw. We measured an average displacement in the back to front axis of 14 μ m and 20 μ m in the left to right axis per 500 μ m travel and of 14 μ m per two screw turns in the top to bottom axis (Fig. 9). As far as monetary costs are concerned, the finalized 3D-printed assembly, including 3D-printing resin, screws, and nuts, remains in the single-digit Euro range.

The implantation process was successful at both the surgery and the recording level of the tests. The recorded data had little noise and spikes were clearly distinguishable from the background (Figs. 10 and 11). It is out of the scope for this publication to go deep into electrophysiological quantification, and the results shown here are just for exemplary purposes. In the specific case of these figures, the silicon probe was not inserted chronically into the bird's brain, but lowered into it every session by slowly turning the screw. For our tests, we visualized the signals while turning the drive, in search for a good placement of the probe, using the wired recording setup. Once content with the location,

we recorded wireless data between one to two hours after advancing the probe. At the end of the recording, we checked the signal under wired condition and returned the probe to its initial position, as leaving the probe inside the brain is known to have adverse effects on signal quality in birds (Chettih et al., 2024).

The data displayed in Figs. 10 and 11, was recorded in the Nidopallium caudolaterale (stereotaxic coordinates 5.5 AP, 7.5 ML and 1–5 DV). In this session the microdrive was last moved two hours before, and the silicon probe was implanted 10 days before that. At the time of recording the baseplate had been implanted for three weeks.

The yield of the recordings remained high for multiple sessions and continued to be high after replacing the probe (Fig. 12). Not only was the yield consistent, but the probe contacts also maintained their impedance throughout a multitude of recording sessions (Fig. 13). Within sessions the single units displayed a consistent amplitude, clear waveforms and had very few inter-spike interval violations, demonstrating a very low contamination with signals from other units (Fig. 14). The probe was also successfully replaced after it stopped working and the implant delivered three additional sessions (Fig. 15). Without the implant technique described here, the experiment could not have been completed with this animal, as 8 sessions were insufficient in this specific protocol.

4. Discussion

Overall, our system succeeded in creating a modular approach for electrophysiology, customizable for multiple species and brain regions. All components can be replaced or exchanged with different ones, if necessary, which has been helpful in the development of the system. Freely moving and flying animals pose a high risk of damaging components, indicating the relevance of the system for our model species. Any problems occurring during recording can be assessed under light anaesthesia by reopening the craniotomy and checking for probe or tissue damage without the need for surgical interventions.

The possibility to split up the implantation procedure into multiple steps protects species with less established anesthesia protocols such as corvids from prolonged operations. The first operation encompassing the steps of opening the craniotomy, implanting the baseplate and connector base of the modular system reduces the anesthesia time per procedure. Adding the microdrive, connector and protective cap in a short second surgery is minimally invasive in comparison to a full surgery.

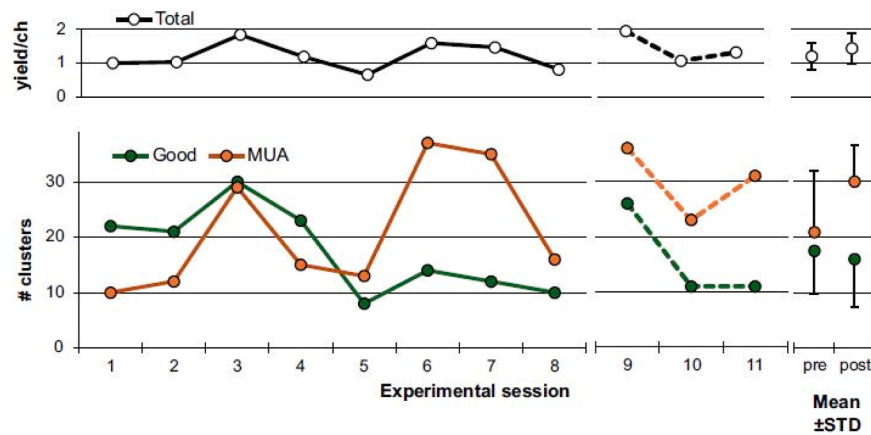


Fig. 12. Cluster count and yield per channel across experimental sessions. At the bottom, the number of clusters obtained after manual curation of the automatic sorter output is represented for each experimental session, for both ‘single units’ (Good, green) and ‘multi unit’ (MUA, orange). Solid lines correspond to sessions 1–8, carried out with one silicon probe, and dashed lines correspond to sessions 9–11, recorded with a second probe. On the right is shown the mean \pm STD for both session series (pre and post). On the top chart, the total yield of clusters per channel (black) is represented for each experimental session in the same way as before. Note that both silicon probes were identical, as explained in the main text, and implanted in the same location. The probe used during sessions 1–8 was first implanted 72 days before session 1, being day 86 after implantation at session 8. The probe for sessions 9–11 was implanted 7 days before session 9, being day 9 after implantation at session 11.

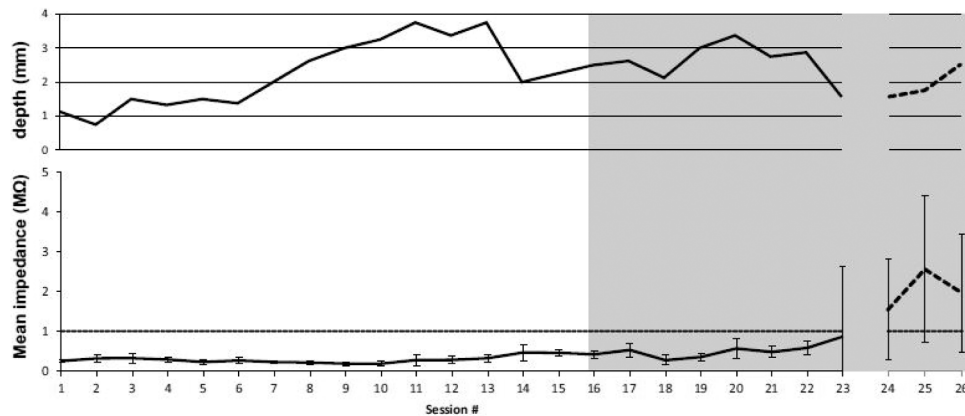


Fig. 13. Probe tip depth and probe mean impedance across sessions. On top, the depth of the tip of the silicon probe is represented, being zero the contact point with the tissue, measured by online signal check while lowering the probe. At the bottom, the mean (\pm STD) impedance at 1 kHz across all 32 channels, measured with INTAN’s dedicated tool for impedance measurement, at the corresponding depth, after a resting period that could vary from 15 min to a necessary time to complete an experimental session. The horizontal line set at $1\text{M}\Omega$ works as reference for a typical impedance where noise floor could make the detection of relatively small amplitude spikes difficult. For both panels, two silicon probes are represented (solid and dashed lines), around the time when they were exchanged. For both panels, the shaded background represents those sessions when experimental sessions were recorded and used on other figures.

A difficulty in in vivo electrophysiology experiments like these is that animals can lose their implants. Implants with imprecise fits pose a higher risk of implant loss as opposed to pure dental cement ones of the same size. A dental cement implant is always an exact mold of the skull, while in all premade implants there is the additional possibility of imperfections in the fixture to the skull. Our implant also has an exact skull fit, which reduces the chance of implant loss. To date, only one of our 17 animals has lost its implant prematurely with the procedure executed as described above. The lost pigeon implant was one of seven implants, involving a head fixation and an above 100mm^2 craniotomy, therefore it had significantly more strain on the connection to the skull. It remains to be seen whether the material causes issues with the use of other species, which is unlikely because it has been used in other studies with rats (Vöröslakos et al., 2021). We are confident that the present approach to design chronic implants should translate well to other common animal models like rodents, as there are not substantial differences that could decrease the stability of the implants. On the contrary, due to less ballistic head movements and a single, dense, unlayered skull bone, we can assume that the implant will be even

sturdier on mammals. No other measures of protection than the common ones are necessary, in our opinion, and the size and weight achieved should work well even for mice.

Frequently mentioned in other publications is the size of the microdrives and, consequently, their weight. Our microdrive has a similar size to the microdrives in other publications with the same or lower microdrive length (Vöröslakos et al., 2021; Caballero-Ruiz et al., 2014; Yang et al., 2008). Regarding the weight, with 150 mg, it is among the lightest microdrives mentioned in the literature. In comparison to other versions, including automatic microdrives, it has fewer components. It is easily removable and can potentially be used multiple times. Our microdrives have low enough divergence from the intended movements for electrophysiology, despite being 3D-printed out of resin. This precision of the microdrive, with its average deflections of $14\text{--}20\text{ }\mu\text{m}$ depending on axis, does not compare to motorized systems (Caballero-Ruiz et al., 2014), but is well above that in other hand turned drives (Ma et al., 2019). The option to place the drive on multiple positions per region allows for more recording sites per implant, a feature that most commercially available implants lack. Positioning the

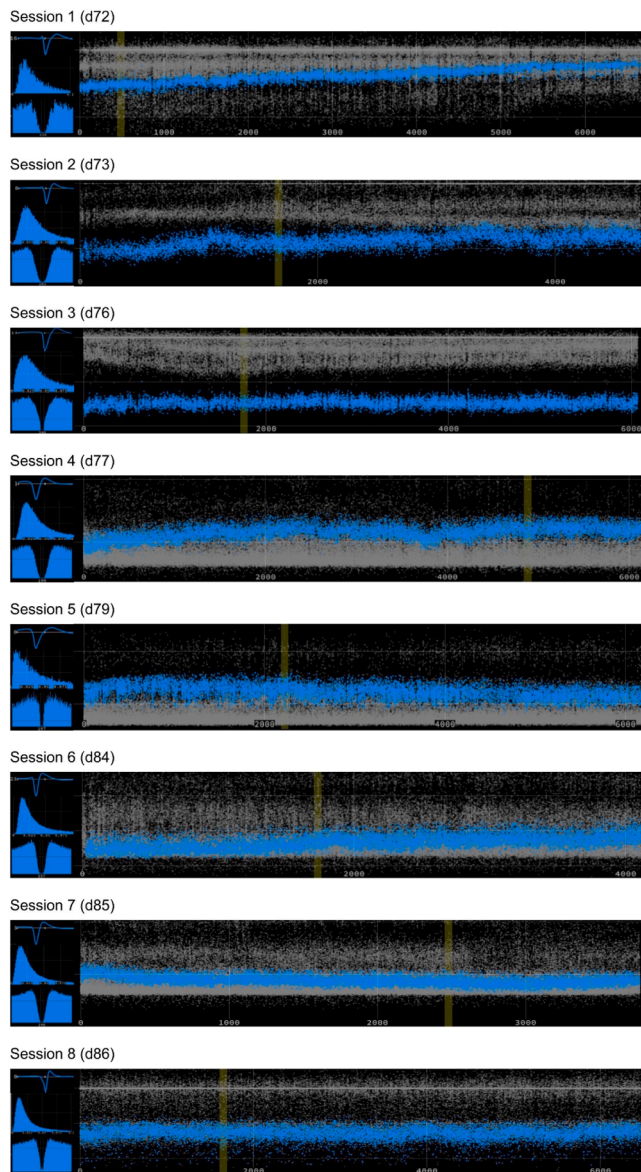


Fig. 14. Mean waveform and basic statistics of one example cluster from sessions 1–8. Eight sessions are represented, one per set of plots. Each session is named in its ordinal occurrence along the experiment and includes the number of days since probe implantation (e.g. d72). Each set shows one example cluster, extracted from the pool of ‘good’ units. The data is shown here as it comes from the visualization and curation software Phy. Each set consists of four panels as follows: on top-left, the mean waveform from all template-matched events, for the channel of maximum amplitude (in arbitrary units for amplitude, and 65 samples of time); on middle-left, the ISI distribution for the same cluster (bins of 0.5 ms, from 0 to 100 ms); on bottom-left, the auto-correlogram for the same cluster (bins of 0.5 ms, from –100–100 ms). On the right, it is shown the first component of the cluster on its temporal and magnitude distribution, as a representation of the ‘drift’ for the cluster along the complete recording session (time in seconds, note that sessions had different durations).

connector base over currently unused craniotomies reduced the spatial footprint of the entire implant.

Lastly, regarding the price and availability of the implant, the current cost of tools and materials enables labs to produce this open-source implant, without relying on outside manufactures for any of the parts besides the probes. As opposed to other implants requiring manufacturing/tools outside of the price/capability range of most labs, like high precision metal 3D-printers, which are therefore supplied by

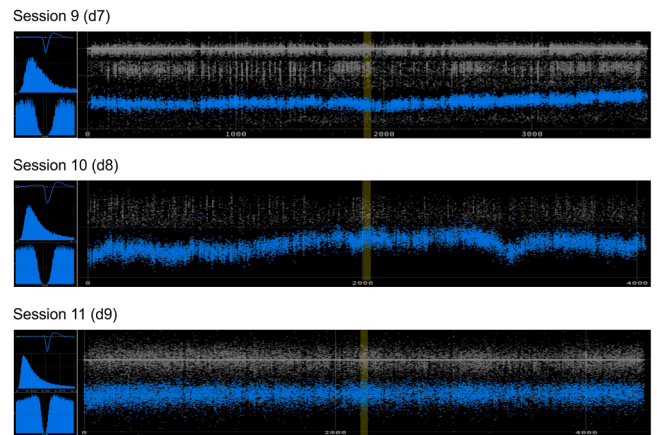


Fig. 15. Mean waveform and basic statistics of three example clusters from sessions 9–11. Exactly as in Fig. 14, but here are shown three sessions after a silicon probe exchange happened, to complete the number of sessions needed for the experimental paradigm. Note that, if this exchange would not have been possible, the 8 previous sessions could be of no use in terms of posterior data analysis.

third parties.

We also ensured that the improvements in operating procedure, production and cost did not come at a reduction in recording quality. The implant with all its additional features still delivers a good recording quality while having added advantages.

Funding

This study was funded by the Deutsche Forschungsgemeinschaft (DFG, German Research Foundation) – Projektnummer 316803389 SFB 1280 (projects A01 & A19).

CRediT authorship contribution statement

Röders Dorian: Writing – original draft, Visualization, Validation, Project administration, Methodology, Investigation, Formal analysis, Data curation, Conceptualization. **Ballesteros Jesus J.:** Writing – review & editing, Validation, Supervision, Project administration, Methodology, Formal analysis, Data curation, Conceptualization. **Sevincik Celil Semih:** Validation, Investigation, Data curation. **Silva Sara Santos:** Writing – review & editing, Validation, Investigation, Formal analysis, Conceptualization. **Bürgel Luca:** Writing – review & editing, Validation, Methodology, Investigation. **Abbas Bilal:** Methodology, Investigation. **Neukirch Yannik:** Investigation. **Pusch Roland:** Writing – review & editing, Project administration, Methodology, Funding acquisition, Conceptualization. **Rose Jonas:** Writing – review & editing, Supervision, Resources, Methodology, Funding acquisition, Conceptualization.

Declaration of Competing Interest

The authors declare no competing interests.

Appendix A. Supporting information

Supplementary data associated with this article can be found in the online version at [doi:10.1016/j.jneumeth.2025.110407](https://doi.org/10.1016/j.jneumeth.2025.110407).

Data availability

Data will be made available on request.

References

- Allen, Leila M., Jayachandran, Maanasa, Viena, Tatiana D., Su, Meifung, McNaughton, Bruce L., Allen, Timothy A., 2020. RatHat: a self-targeting printable brain implant system. *eNeuro* 7 (2). <https://doi.org/10.1523/ENEURO.0538-19.2020>.
- Bilkey, David K., Russell, Noah, Colombo, Michael, 2003. A lightweight microdrive for single-unit recording in freely moving rats and pigeons. *Methods* 30 (2), 152–158. [https://doi.org/10.1016/S1046-2023\(03\)00076-8](https://doi.org/10.1016/S1046-2023(03)00076-8).
- Buzsáki, György, 2004. Large-scale recording of neuronal ensembles. *Nat. Neurosci.* 7 (5), 446–451. <https://doi.org/10.1038/nn1233>.
- Caballero-Ruiz A.; L.I. Garcia-Beltran; L. Ruiz-Huerta; F. Heredia-Lopez (2014): Micropositioning System for the Study of Neural Activity in Free-Behaving Rats. In: 2014 International Conference on Mechatronics, Electronics and Automotive Engineering. 2014 International Conference on Mechatronics, Electronics and Automotive Engineering, pp. 168–172.
- Chettih, Selmaan N., Mackevicius, Emily L., Hale, Stephanie, Aronov, Dmitriy, 2024. Barcoding of episodic memories in the hippocampus of a food-caching bird. *Cell* 187 (8), 1922–1935.e20. <https://doi.org/10.1016/j.cell.2024.02.032>.
- Guillory, K.S., Normann, R.A., 1999. A 100-channel system for real time detection and storage of extracellular spike waveforms. *J. Neurosci. Methods* 91 (1-2), 21–29.
- Jones, Marc E.H., Button, David J., Barrett, Paul M., Porro, Laura B., 2019. Digital dissection of the head of the rock dove (*Columba livia*) using contrast-enhanced computed tomography. *Zool. Lett.* 5 (1), 17. <https://doi.org/10.1186/s40851-019-0129-z>.
- Jun, James J., Steinmetz, Nicholas A., Siegle, Joshua H., Denman, Daniel J., Bauza, Marius, Barbarits, Brian, et al., 2017. Fully integrated silicon probes for high-density recording of neural activity. *Nature* 551 (7679), 232–236. <https://doi.org/10.1038/nature24636>.
- Lewis, David I., 2019. Animal experimentation: implementation and application of the 3Rs. *Emerg. Top. Life Sci.* 3 (6), 675–679. <https://doi.org/10.1042/ETLS20190061>.
- Ma, Jun, Zhao, Zifang, Cui, Shuang, Liu, Feng-Yu, Yi, Ming, Wan, You, 2019. A novel 3D-printed multi-drive system for synchronous electrophysiological recording in multiple brain regions. *Front. Neurosci.* 13, 1322. <https://doi.org/10.3389/fnins.2019.01322>.
- Pachitariu, Marius; Steinmetz, Nicholas; Kadir, Shabnam; Carandini, Matteo; Kenneth D., Harris (2016): Kilosort: realtime spike-sorting for extracellular electrophysiology with hundreds of channels.
- Overton, Jacqueline A., Cooke, Dylan F., Goldring, Adam B., Lucero, Steven A., Weatherford, Conor, Recanzone, Gregg H., 2017. Improved methods for acrylic-free implants in nonhuman primates for neuroscience research. *J. Neurophysiol.* 118 (6), 3252–3270. <https://doi.org/10.1152/jn.00191.2017>.
- Pomberger, Thomas, Hage, Steffen R., 2019. Semi-chronic laminar recordings in the brainstem of behaving marmoset monkeys. *J. Neurosci. Methods* 311, 186–192.
- Psarou, Eleni, Vezoli, Julien, Schölvinck, Marieke L., Ferracci, Pierre-Antoine, Zhang, Yufeng, Grothe, Iris, et al., 2023. Modular, cement-free, customized headpost and connector-chamber implants for macaques. *J. Neurosci. Methods* 393, 109899. <https://doi.org/10.1016/j.jneumeth.2023.109899>.
- Pusch, Roland, Julian, Packheiser, Amir Hossein, Azizi, Celil Semih, Sevincik, Jonas, Rose, Sen, Cheng, et al., 2023. Working memory performance is tied to stimulus complexity. *Commun. Biol.* 6 (1), 1119. <https://doi.org/10.1038/s42003-023-05486-7>.
- Rose, Jonas, 2018. Chapter 11 - Neurophysiology Techniques in the Avian Brain: Single Units and Field Recordings. In: Manahan-Vaughan, Denise (Ed.), *Handbook of Behavioral Neuroscience: Handbook of Neural Plasticity Techniques*, 28. Elsevier, pp. 213–221. (<https://www.sciencedirect.com/science/article/pii/B9780128120286000112>) (Available online at).
- Steinmetz, Nicholas A., Koch, Christof, Harris, Kenneth D., Carandini, Matteo, 2018. Challenges and opportunities for large-scale electrophysiology with neuropixels probes. *Curr. Opin. Neurobiol.* 50, 92–100. <https://doi.org/10.1016/j.conb.2018.01.009>.
- Yang, Sungwook; Lee, Semin; Park, Kitae; Jeon, Hyojin; Huh, Yeowool; Cho, Jeiwon et al. (2008): Piezo motor based microdrive for neural signal recording. In Annual International Conference of the IEEE Engineering in Medicine and Biology Society. IEEE Engineering in Medicine and Biology Society. Annual International Conference 2008, pp. 3364–3367.
- Voigts, Jakob, Siegle, Joshua H., Pritchett, Dominique L., Moore, Christopher I., 2013. The flexDrive: an ultra-light implant for optical control and highly parallel chronic recording of neuronal ensembles in freely moving mice. *Front. Syst. Neurosci.* 7, 8. <https://doi.org/10.3389/fnsys.2013.00008>.
- Vöröslakos, Mihály, Petersen, Peter C., Vöröslakos, Balázs, Buzsáki, György, 2021. Metal microdrive and head cap system for silicon probe recovery in freely moving rodent. *eLife* 10. <https://doi.org/10.7554/eLife.65859>.